



Research Article

Renewable Energy Based Smart Grid Construction Using Hybrid Design in Control System with Enhancing of Energy Efficiency of Electronic Converters for Power Electronic in Electric Vehicles

Suhasini Sodagudi,¹ C Manjula,² M. S. Vinmathi,³ R. Shekhar,⁴ José Luis Arias Gonzáles,⁵ C. Ramesh Kumar,⁶ Gaurav Dhiman ^{7,8,9} and A. R. Murali Dharan ¹⁰

¹Department of IT, Velagapudi Ramakrishna Siddhartha Engineering College, Kanuru, AP, India

²Department of Mechatronics, The Oxford College of Engineering, Bommanahalli, Bengaluru, India

³CSE Department, Panimalar Engineering College, Bangalore Trunk Road, Nazarethpet, Poonamallee, Chennai, India

⁴Department of Computer Science and Engineering, Alliance University, Bangalore, India

⁵Pontificia Universidad Católica Del Peru, Lima, Peru

⁶School of Computing Science and Engineering, Galgotias University, Greater Noida, Uttar Pradesh, India

⁷Department of Electrical and Computer Engineering, Lebanese American University, Byblos, Lebanon

⁸University Centre for Research and Development, Department of Computer Science and Engineering, Chandigarh University, Gharuan-140413, Mohali, India

⁹Department of Project Management, Universidad Internacional Iberoamericana, Campeche, Mexico

¹⁰Debre Berhan University, Debre Berhan, Ethiopia

Correspondence should be addressed to A. R. Murali Dharan; mdharan75@dbu.edu.et

Received 6 July 2022; Accepted 25 August 2022; Published 4 October 2022

Academic Editor: R Sitharthan

Copyright © 2022 Suhasini Sodagudi et al. This is an open access article distributed under the Creative Commons Attribution License, which permits unrestricted use, distribution, and reproduction in any medium, provided the original work is properly cited.

The power electronic interface is critical in matching a distributed generation (DG) unit's characteristics to grid requirements as most DG technologies rely on renewable energy. Increased adoption of electric vehicles (EV) is seen as a positive step toward minimizing air pollution as well as carbon emissions. Rapid proliferation of electric vehicles as well as charging stations has exacerbated voltage quality as well as harmonic distortion difficulties, which harm the efficiency of combined renewable energy. This research proposes novel hybrid design techniques in control systems that enhance the energy efficiency of electronic converters for power electronics. The control system enhancement has been carried out using a hybrid energy storage electric converter, and energy efficiency is improved using a synergetic battery reference adaptive controller. A plug-in hybrid electric vehicle (PHEV)'s internal combustion engine with a small photovoltaic (PV) module is utilised to assess a proposed control method which effectively regulates electric power on-grid by draining electricity from batteries during peak hours as well as then charging them during off-peak times, lowering the load on the converter as well as allowing electric vehicles to charge faster. Experimental results show the constant acceleration case obtained battery current of 92 Amps, ultracapacitor current of 89 Amps, charging voltage of 88 V, DC load current of 85 Amps, battery SOC of 72%, and the time-varying acceleration proposed technique obtained current of 94 Amps, and ultracapacitor current of 90 Amps, charging voltage of 90 V, DC load current of 82 Amps, battery SOC of 79%.

1. Introduction

Traditional power systems use enormous power producing units that are geographically scattered to produce the

majority of power, which is then routed to large consumption centres as well as distributed to various clients. This composition has begun to shift toward new scenarios in which DG units are scattered across distribution networks

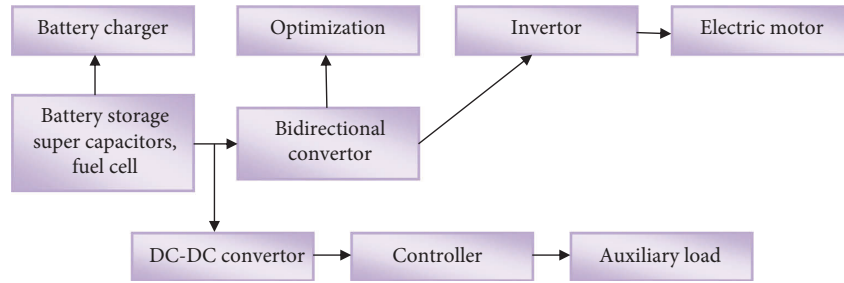


FIGURE 1: Architecture of interfacing and application of power electronic converters.

[1]. Wind turbines, photovoltaics, fuel cells, biomass, tiny hydro-plants, and other renewable resources are used in these DGs [2]. Through quick and efficient PE converters and sustainable are linked to the smart grid (SG) for the advanced data collection infrastructure [3]. Plug-in HEVs (PHEVs) have been offered as a possible alternative because the charging efficiency of CS mode is primarily dependent on regenerative braking and gasoline. Unlike HEVs, PHEVs can also be charged externally using power outlets [4]. The majority of power in a PHEV comes from an EM, which serves as the primary source of power, with ICE serving as a backup. When battery SOC reaches a certain level, the PHEV switches to a standard HEV mode, and ICE becomes the primary power source. PHEVs have extended all-electric range, better local air quality as well as ability to connect to the grid [5]. The efficient performance of EVs depends on perfect synchronisation between ESs as well as power electronic converters. The primary picture of an EV in Figure 1 helps to understand the application as well as the interfacing of ESs and power electronic converters in EVs.

To build the internal structure of EVs, ESs types such as supercapacitors, batteries, and fuel cells, are combined with power electronic converters/inverters. ESs are protected from stray current harm by the inverter, which also functions as a motor controller as well as a filter. ESs delivers electricity with unstable characteristics and large voltage drops. It is efficiently addressed by DC-DC converters [6].

Contribution of this paper is as follows:

- (1) To propose novel technique in hybrid design in control system with enhancing the energy efficiency of electronic converters for power electronic
- (2) To develop control system enhancement has been carried out using a hybrid energy storage electric convertor and energy efficiency has been improved using a Synergetic battery reference adaptive controller.
- (3) Designing a PHEV's internal combustion engine with a tiny photovoltaic (PV) module.

2. Related Works

HESS is primarily dependent on personal judgement and experience [7]. Researchers are experimenting with various combinations of energy sources to build an efficient HESS for HEVs. In HEVs, energy storage methods have primary

and secondary energy sources [8]. The most prevalent fuel cell batteries are fuel cell-supercapacitor, battery-supercapacitor, and cell photovoltaic panels [9]. The primary energy source gives a long driving range, while the secondary energy source is only used when abrupt acceleration or braking is required [10]. The FC's high cost, as well as low power density, are two key drawbacks that prevent it from being utilised as an energy source. A supercapacitor (SC) is used as a supplementary energy source to balance the load from an FC [11]. SC's fundamental flaw is that it has a poor energy density [12]. [13] presented a battery-supercapacitor HESS; lithium-ion batteries' main drawbacks are their high cost as well as low energy density. Another stumbling block is that consumers must change batteries regularly, increasing the expense of HEVs. SC is utilised to capture energy loss as well as charge batteries in FC cars. A combined derived boost as well as a fly back converter design are presented [14] to achieve high voltage gain in fuel cell-based HEVs. A cascaded multiport converter for switching reluctance motors has been proposed for battery management as well as DC bus voltage adjustment [15]. A bidirectional DC-DC interleaved converter based on optimization is described [16] to minimize overshoots/undershoots in optimised switching functions. MIMO converters, as well as single bidirectional converter topologies, are introduced in HEVs. In the literature, numerous control methods for energy management as well as control of HEVs are proposed [17]. A GA-based fuzzy logic controller has been developed to increase the performance as well as fuel economy of fuel cell-based HEVs [18]. To manage power as well as maintain level of charge in battery, an adaptive fuzzy logic based controller for fuel energy management as well as battery-based HEVs was utilised [19]. To increase battery performance and prevent battery as well as fuel cell degradation, a predictive controller method has been introduced [20]. The energy management method in fuel cell vehicles includes a robust fuzzy model predictive controller [21, 22]. The most common type of main storage unit is lithium-ion batteries. Thermal runaway behaviour of lithium-ion batteries after overcharging is greatly influenced by diverse cell packaging configurations [23]. Furthermore, battery age prediction is required for the smooth as well as effective operation of coupled battery methods in electric cars. HESS's appropriate sizing is critical for increasing efficiency as well as extending the life of storage parts. The authors of [24] explore a multi-objective method for optimising overcharging aim as well as lowering

the system's cost. Because UC has a higher power density than battery, a combination of battery as well as ultra-capacitor (UC) may be a preferable solution [25]. The overall system performance will be cost-effective in a combined battery-UC-based HESS model, while battery life will be extended. Multiple control solutions are given in the literature; however, they all have localised control limits [26].

3. System Model

Environmental variables as well as load changes are studied to carry out renewable energy transmission on a transmission method. Environmental conditions, synchronisation and overloading are the main causes of renewable energy transmission uncertainties. Overloading and other forms of fluctuations wreak havoc on a network's performance.

A suggested hybrid energy storage technique made up of a DC/DC converter, super capacitors, and a Li-ion battery is shown in Figure 2. The battery pack powers the smooth DC motor. A sudden state of peak power supply is dealt with by the supercapacitor. The electric vehicle's power management system determines the flow of electrical energy based on the load demand.

Hybrid energy storage electric convertor (HESEC):

Physical, chemical, and EM energy storage devices are three types of energy storage devices. The essential speciation of most common energy storage devices is listed in Table 1.

Table 1 illustrates that a single energy storage device cannot unite power density and energy density and meet complex and variable power demands of electric vehicles. It is proposed that batteries as well as supercapacitors are employed to manage the EV power supply fluctuations. The battery's high energy density ensures the EV range on a single charge, and the SCs can deliver a burst of high current to satisfy the peak power demands of electric vehicles, providing dynamic performance. The SC can absorb feedback energy more efficiently and quickly, improving the system's energy efficiency and protecting the battery from excessive current. A new power allocation approach is charging as well as discharging of the battery and SC.. The bidirectional DC/DC converter has a half-bridge architecture. A supercapacitor is an energy storage device that holds electric energy derived from various renewable energy sources. It's usually separated into two categories: piled and wound. The materials used in the electrodes have a significant impact on the energy storage capabilities of SCs. A spiral-wrapped SC with ordered mesoporous carbon electrodes was utilised in this investigation. The SC structure is depicted in Figure 3.

A cascade voltage as well as a current controller are chosen to maintain a consistent load voltage. Super-capacitors can respond more quickly and recycle braking energy when the DC side voltage rises significantly during braking. The supercapacitor controller's control structure is given in Figure 3.

V_{dc} and V_{dc-sen} are actual as well as rated voltages of a DC motor, respectively; * UC I and * UC sen I are per unit

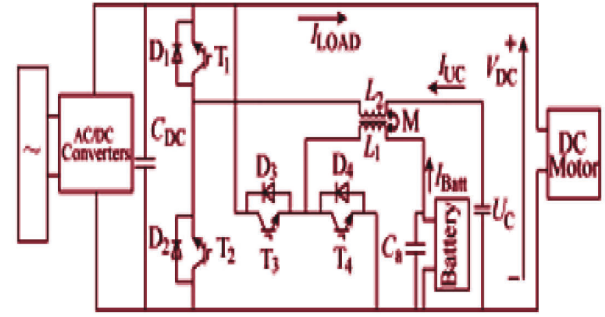


FIGURE 2: Topology of the hybrid energy storage structure.

actual and rated currents of a super-capacitor, respectively; f_s is switching frequency, and $G_{1,2}$ are switching signals of T_1 and T_2 . Duty cycle of the inductor current transfer function in boost mode is represented as :

$$\frac{I_{L2}(s)}{D(s)} = \frac{V_{dc}R_{Load}C_{dc}s + 2V_{dc}}{R_{Load}L_2C_{dc}s^2 + L_2s + R_{Load}(1-D)^2} \quad (1)$$

The reference current of L_2 is $IL2(s)$, the DC motor voltage is V_{dc} , the capacitor DC motor is C_{dc} , and the duty cycle is D .

In contrast to the nonisolated DC/DC converter used earlier, the DC/DC converter utilizes a composite converter with an isolated soft switch. Switching to an isolated converter during a rapid rise in current can protect the energy storage system from harm caused by direct electrical connections. Figure 4 shows how the DC/DC converter performs in the boost method during discharge as well as buck mode during energy feedback under normal working conditions.

This research utilizes an E-type magnetic core to achieve magnetic element integration. A coupling inductance (L_1 and L_2) is employed in this example. L_2 is output filter inductor, L_1 is external inductance, and C_a is the extra capacitance, as illustrated in Figure 5. C_a 's voltage is identical to the output voltages of L_2 and L_1 in steady-state, regardless of the capacitor voltage ripple. Figure 4 shows a DC/DC converter with four IGBT switches ($T_1 \sim T_4$) and four diodes ($D_1 \sim D_4$). Two operating modes for a boost converter and three operational modes for a buck converter. Furthermore, output current ripple is minimized by using an integrated magnetic design.

In order to highlight the operating principle of the proposed HESEC, reference should be made to overall DC-link voltage and energy time-variations. These can be achieved based on (2) and (3):

$$C_{DC} \frac{dV_{DC}}{dt} = i_B - i_{DC}, i_{DC} = c_H i_H + c_L i_L, \quad (2)$$

$$\frac{dE_{DC}}{dt} = V_{DC}(i_B - i_p), i_p = v_H i_H + v_L i_L. \quad (3)$$

IDC and i_p are equivalent DC-link and power currents, proportional to the power exchanged by the DC-link and the electrical drive, respectively. Referring to (5), CDC denotes

TABLE 1: Main specifications of common energy storage.

Energy storage type	Energy density (Wh/kg)	Efficiency (%)	Service cycle	Power density (W/kg)	Cost (\$/kW/Year)
Battery	30 – 240	60 – 80	≤ 2000	100 – 700	25 – 120
Supercapacitor	≤ 10	≥ 90	$\geq 10^5$	700 – 18,000	85
Lithium battery	250 – 300	≥ 85	$10^3 - 10^4$	800 – 1100	120
Superconducting energy storage	≤ 10	≥ 95	$\geq 10^5$	$\geq 10^4$	200

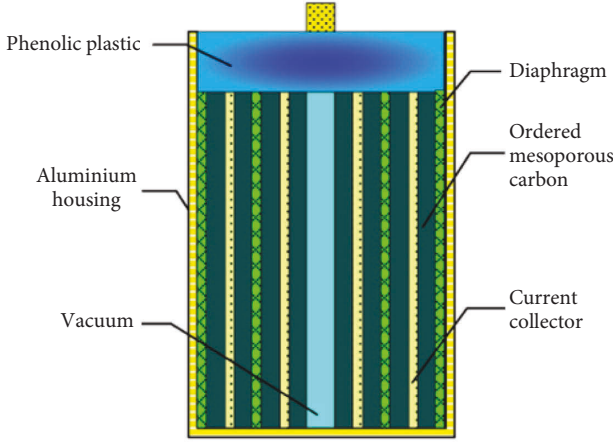


FIGURE 3: SC Structure diagram.

equivalent DC-link series capacitance, whereas c_H and c_L are per unit capacitances in

$$C_{DC} = \frac{C_H C_L}{C_H + C_L}, c_H = \frac{C_H}{C_H + C_L}, c_L = \frac{C_L}{C_H + C_L}. \quad (4)$$

Similarly, v_H and v_L reported in (5) represent the per unit capacitor voltages:

$$v_H = \frac{V_H}{V_H + V_L}, v_L = \frac{V_L}{V_H + V_L}. \quad (5)$$

Still referring to both (4) and (5), it can be stated that VDC and EDC can be varied independently if suitable combinations of (c_H, c_L) and (v_H, v_L) occur. As a result, the DC-link energy content can be changed without affecting the overall DC-link voltage: this is the fundamental concept based on which the proposed HESEC is developed. To corroborate the previous statement, DC-link energy base value can be introduced as

$$E'_{DC} = \frac{1}{2} C_L V_{DC}^2. \quad (6)$$

Therefore, dividing (4) by (6), per unit energy content of DC-link is easily attained as (7) where in which ζ denotes the unbalance capacitance factor (8):

$$e_{DC} = \zeta v_H^2 + (1 - v_u)^2, \quad (7)$$

$$\zeta = \frac{C_H}{C_L}. \quad (8)$$

Hence, DC-link voltage unbalances can be usefully introduced by varying the UC voltage within a given range, thus varying the overall DC-link energy content without

affecting its overall voltage. As a result, appropriate DC-link energy and voltage regulations enable optimal energy flow management among each HESEC component.

4. Synergetic Battery Reference Adaptive Controller (SBRAC)

The PHEV model was developed by utilizing basic electric current as well as voltage rules across energy sources and power converters. The speed of an induction motor whose load torque is directly connected with rotor flux is controlled using a field oriented control technique. The circuit diagram of PHEV's unified method is represented in Figure 6.

To overcome all of the difficulties above and achieve our desired response, an approach based on adaptive terminal sliding management of PHEV is provided. The general flow of PHEVs is depicted in Figure 7, which includes a charging unit, battery, mutual DC bus, UC bank, and load. An unregulated bridge rectifier and a DC-DC buck converter are connected to the mains supply to improve the charge of the battery using the charger. Bidirectional DC-DC buck-boost converters are utilised in the HESS model to connect the PHEV's power sources to the DC voltage line. The complete PHEV control system is split into two levels:

Low-level control: This entails controlling power converters to regulate the DC bus and allowing current to flow in both directions at a localised level.

The increased demand for PHEVs necessitates the development of an integrated charging source for vehicles. The smart charger's integration with the PHEV is the most cost-effective approach. As the number of HEVs on the road grows, so does demand, which has a significant influence on the power distribution method of power factor correction as well as harmonic oscillations. Here, battery voltage is a defined function of the SoC and is represented as

$$S = \frac{Ch}{Ch_{nom}}, \quad (9)$$

where S is SoC, Ch is the battery's absolute capacity in "Ah," and Ch_{nom} is the battery's nominal "Ah" capacity. Following (10) and (11) are utilised to detect fact of active and reactive grid powers during charging method of a PHEV.

$$P_{grid}(S) = VI \cos \phi(S), \quad (10)$$

$$P_{grid}(S) = VI \sin \phi(S), \quad (11)$$

where P_{grid} is the grid power, ϕ is the power factor, and V and I are grid voltage and current. Consider charging source's effectiveness, DC voltage is represented in AC power as

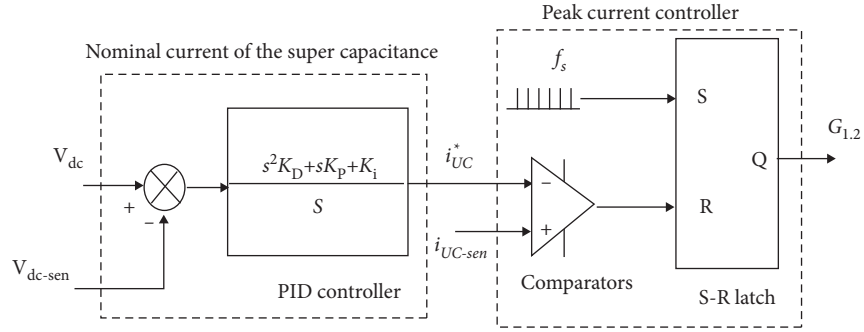


FIGURE 4: Topology of a DC/DC converter with an integrated magnetic structure.

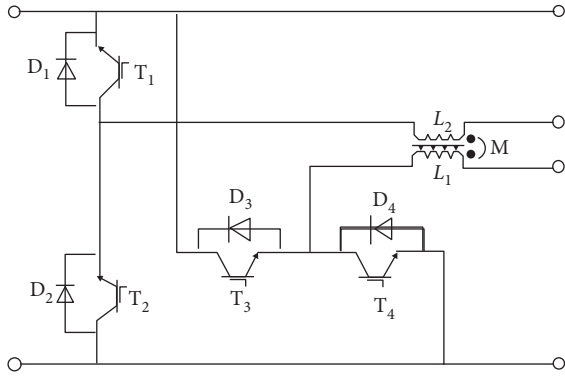


FIGURE 5: Block diagram of the supercapacitor voltage and current controller.

source, as directed by the high level controller, provides instantaneous power to the battery linked in a HESS method of controlled buck converter is constructed, as shown in (13) and (14):

$$\frac{dx_1}{dt} = \frac{V_g}{L_1}u_1 - \frac{x_2}{L_1}, \quad (13)$$

$$\frac{dx_2}{dt} = \frac{x_1}{C_1} - \frac{V_g}{R_1C_1}u_1, \quad (14)$$

where x_1 is average inductor current I_{L1} , x_2 is average output.

5. Performance Analysis

Simulations on MATLAB/Simulink were used to test the validity of all of the suggested controllers, which were subjected to the normal European extra urban driving cycle to guarantee that the necessary control objectives were met. Tables 2–4 provide detailed information on energy sources, 3-phase induction, motors power converters and vehicle under consideration. Proposed controllers' design parameters were chosen using a hit-and-miss approach. Table 5 shows the parameters of the HESEC model.

The above Table 6 shows comparative analysis based on constant acceleration and time-varying acceleration cases. Here the parameters compared are battery current, ultracapacitor current, charging voltage, DC load current, and battery SOC. All the parameters have been analysed based on hybrid design in control systems enhancing the energy efficiency of electronic converters for power electronics.

The above Figures 9 and 10 show comparative analysis of constant acceleration and time-varying acceleration case. Here for both cases, the proposed technique obtained optimal results in developing hybrid designs in control system while enhancing the energy efficiency of electronic converters for power electronics. The proposed technique in the constant acceleration case obtained a battery current of 92 Amps, ultracapacitor current of 89 Amps, charging voltage of 88 V, DC load current of 85 Amps, battery SOC of 72%; while the existing technique HESS obtained battery current of 88 Amps, ultracapacitor current of 82 Amps, charging voltage of 81 V, DC load current of 70 Amps, battery SOC of 65%; HEV obtained battery current of 88 Amps, ultracapacitor current of 82 Amps, charging voltage of 81 V, DC

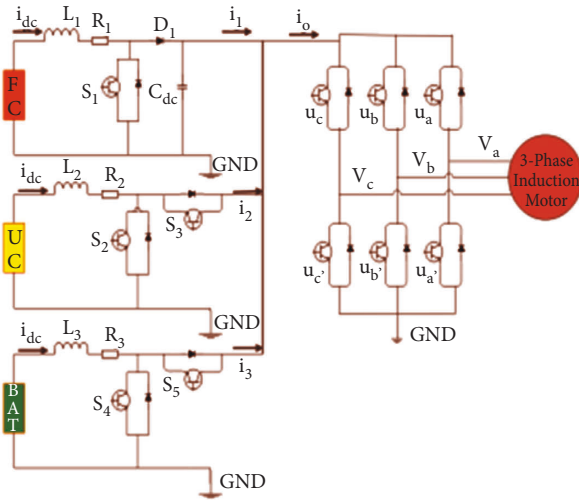


FIGURE 6: Electric circuit diagram of PHEV.

$$P_{ch}(S) = \eta[VI \cos \phi(S)], \quad (12)$$

where, η is the charging source's efficiency and P_{ch} is the charger's power. An integrated charging source has been modelled in this section, which comprises an AC supply linked with a boost converter and a regulated buck converter, as shown in Figure 8. Furthermore, an adaptive nonlinear controller was developed to manage charge flow and estimate unknown parameters (R_1 , C_1). The charging

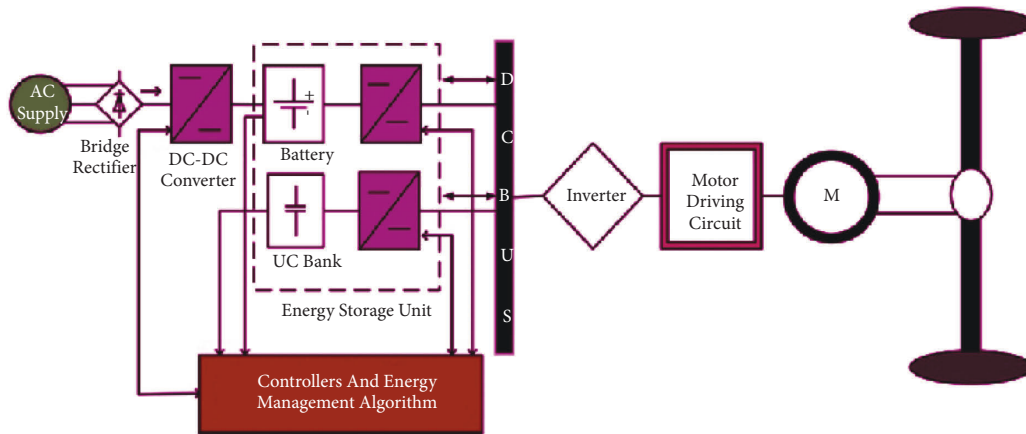


FIGURE 7: General block diagram of PHEV.

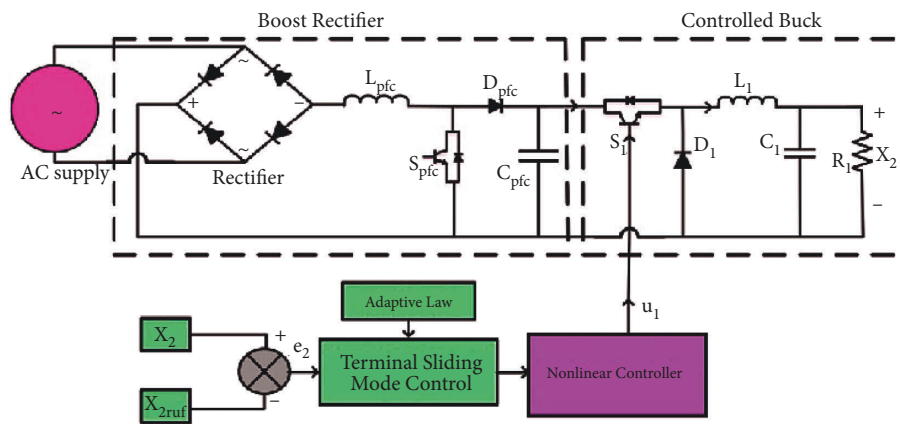


FIGURE 8: Integrated charging unit for PHEV.

TABLE 2: Energy sources data.

Sources	Specifications
Fuel cell (PEMFC)	34 KW, 350 V, 250 A
Battery	288 Vdc, 13.9 Ah, Li-on
Ultracapacitor	2700 F, 250 Vdc

TABLE 3: Power converters data.

Parameters	Specifications
Switching frequency (F_s)	20 kHz
Resistances R_1, R_2 and R_3	20 m Ω
Output capacitance (C_{out})	1.66 mF
Inductances L_1, L_2 and L_3	3.3 mH

TABLE 4: Parameters of smart charging source.

AC grid nominal voltage	230 V
Inductance L_1	10 mH
Frequency	50 Hz
Capacitor C_1	1 mF
Resistance R_1	15 m Ω

TABLE 5: Parameters of HESEC model.

Battery(Li-ion)	230 V/13.9 Ah
UC module	205 V/2700 F
Inductances L_2, L_3	100 mH
Switching frequency	100 KHz
Output capacitor C_{dc}	10 mF
Parasitic resistances $R_2, R_3,,$	20 m Ω

load current of 70 Amps, battery SOC of 65%. In case of time-varying acceleration proposed technique obtained current of 94 Amps, ultracapacitor current of 90 Amps, charging voltage of 90 V, DC load current of 82 Amps, battery SOC of 70%; while the existing technique HESS obtained battery current of 90 Amps, ultra-capacitor current of 85 Amps, charging voltage of 85 V, DC load current of 68 Amps, battery SOC of 74%; HEV obtained battery current of 92 Amps, ultra-capacitor current of 89 Amps, charging voltage of 89 V, DC load current of 78 Amps, battery SOC of 79%. From the above analysis, the proposed technique obtained optimal results in enhancing the energy efficiency of electronic converters for power electronics.

TABLE 6: Comparative analysis is based on the constant acceleration case and the time varying acceleration case.

Cases	Techniques	Battery current	Ultra capacitor current	Charging voltage	DC load current	Battery SOC
Case 1	HES	88	82	81	70	65
	HEV	91	86	85	80	69
	HESEC_SBRAC	92	89	88	85	72
Case 2	HES	90	85	85	68	70
	HEV	92	89	89	78	74
	HESEC_SBRAC	94	90	90	82	79

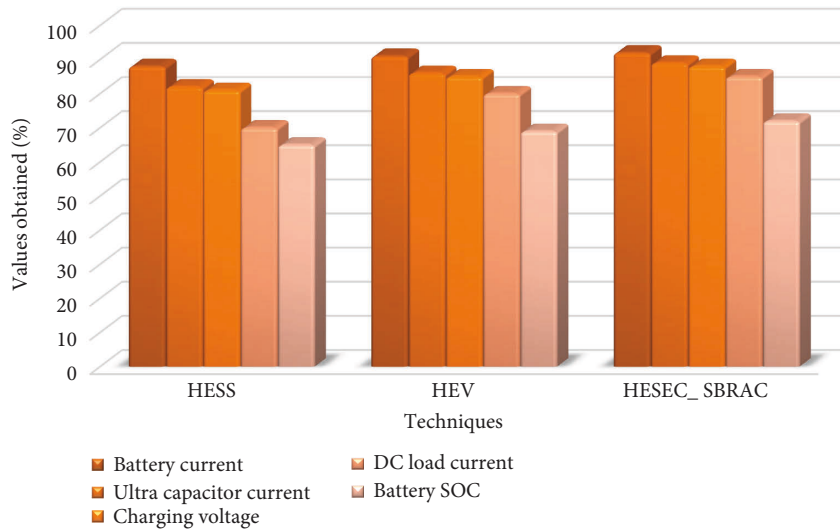


FIGURE 9: Comparative analysis of the constant acceleration case.

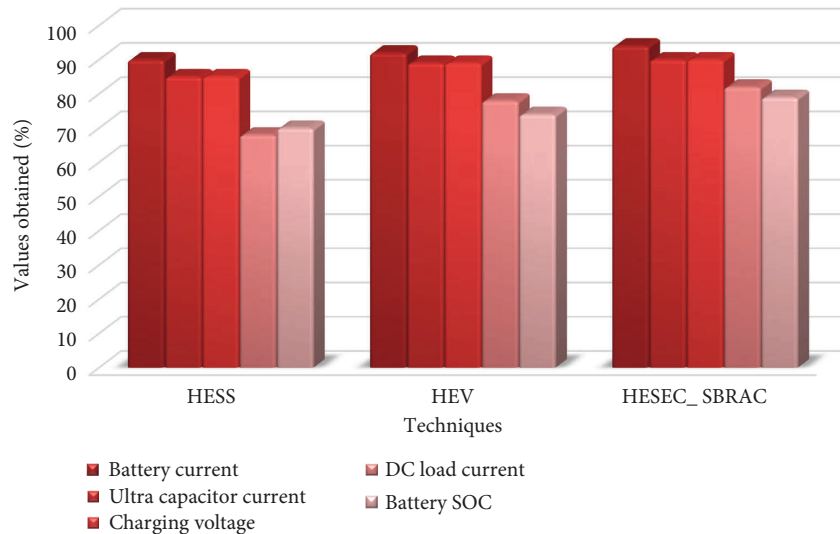


FIGURE 10: Comparative analysis of the constant acceleration case.

6. Conclusion

This research proposed a novel technique in hybrid design in control systems to enhance the energy efficiency of electronic converters for power electronics. Here the control system enhancement has been carried out using a hybrid

energy storage electric convertor and energy efficiency is improved using a synergetic battery reference adaptive controller. A PHEV’s internal combustion engine with a small photovoltaic (PV) module is shown here. The effectiveness of the suggested control system’s energy management is evaluated using simulations. By drawing power from

batteries during peak hours and then recharging them during off-peak hours, the suggested method efficiently manages the grid's supply of electricity. This reduces the load on the converter and enables electric vehicles to charge more quickly. Regardless of changes in renewable energy supply and load, the system maintains a steady voltage. Experimental results show Constant acceleration case obtained battery current of 92 Amps, ultra-capacitor current of 89 Amps, charging voltage of 88 V, DC load current of 85 Amps, battery SOC of 72% and time-varying acceleration proposed technique obtained current of 94 Amps, ultra-capacitor current of 90 Amps, charging voltage of 90 V, DC load current of 82 Amps, battery SOC of 79%.

Data Availability

The data will be available by corresponding author upon request.

Conflicts of Interest

The authors declare that they have no conflicts of interest.

References

- [1] D. Yuan, M. Sun, M. Zhao et al., "Persulfate promoted ZnIn₂S₄ visible light photocatalytic dye decomposition," *International Journal of Electrochemical Science*, vol. 15, pp. 8761–8770, 2020.
- [2] X. Feng, Y. Zhang, L. Kang et al., "Integrated energy storage system based on triboelectric nanogenerator in electronic devices," *Frontiers of Chemical Science and Engineering*, vol. 15, no. 2, pp. 238–250, 2020.
- [3] C. Y. Bu, F. J. Li, K. Yin, J. B. Pang, L. C. Wang, and K. Wang, "Research progress and prospect of triboelectric nanogenerators as self-powered human body sensors," *ACS Appl. Electron. Mater.* vol. 2, no. 4, pp. 863–878, 2020.
- [4] G. T. Xia, Y. N. Huang, F. J. Li et al., "A thermally flexible and multi-site tactile sensor for remote 3D dynamic sensing imaging," *Frontiers of Chemical Science and Engineering*, vol. 14, no. 6, pp. 1039–1051, 2020.
- [5] W. L. Wang, Y. H. Li, L. W. Li, L. C. Wang, and K. Wang, "Nanoparticle structure for flexible quasi-solid-state lithium-ion batteries," *International Journal of Electrochemical Science*, vol. 15, pp. 1–14, 2020.
- [6] S. Ansari, A. Ayob, M. S. Hossain Lipu, A. Hussain, and M. H. M. Saad, "Multi-channel profile based artificial neural network approach for remaining useful life prediction of electric vehicle lithium-ion batteries," *Energies*, vol. 14, no. 22, 2021.
- [7] F. Mumtaz, N. Zaihar Yahaya, S. Tanzim Meraj, B. Singh, R. Kannan, and O. Ibrahim, "Review on non-isolated DC-DC converters and their control techniques for renewable energy applications," *Ain Shams Engineering Journal*, vol. 12, no. 4, pp. 3747–3763, 2021.
- [8] C. Akkaldevi, S. D. Chitta, J. Jaidi, S. Panchal, M. Fowler, and R. Fraser, "Coupled electrochemical-thermal simulations and validation of minichannel cold-plate water-cooled prismatic 20 ah LiFePO₄ battery," *Electrochemistry (Tokyo, Japan)*, vol. 2, no. 4, pp. 643–663, 2021.
- [9] K. Purohit, S. Srivastava, V. Nookala et al., "Soft sensors for state of charge, state of energy, and power loss in formula student electric vehicle," *Applied System Innovation*, vol. 4, pp. 78–85, 2021.
- [10] V. G. Choudhari, A. S. Dhoble, S. Panchal, M. Fowler, and R. Fraser, "Numerical investigation on thermal behaviour of 5 × 5 cell configured battery pack using phase change material and fin structure layout," *Journal of Energy Storage*, vol. 43, Article ID 103234, 2021.
- [11] K. Liu, Z. Yang, X. Tang, and W. Cao, "Automotive battery equalizers based on joint switched-capacitor and buck-boost converters," *IEEE Transactions on Vehicular Technology*, vol. 69, no. 11, pp. 12716–12724, 2020.
- [12] Y. Shang, K. Liu, N. Cui, N. Wang, K. Li, and C. Zhang, "A compact resonant switched-capacitor heater for lithium-ion battery self-heating at low temperatures," *IEEE Transactions on Power Electronics*, vol. 35, no. 7, pp. 7134–7144, 2020.
- [13] Y. Shang, K. Liu, N. Cui, Q. Zhang, and C. Zhang, "A sine-wave heating circuit for automotive battery self-heating at subzero temperatures," *IEEE Transactions on Industrial Informatics*, vol. 16, no. 5, pp. 3355–3365, 2020.
- [14] K. Liu, X. Hu, H. Zhou, L. Tong, W. D. Widanage, and J. Marco, "Feature analyses and modeling of lithium-ion battery manufacturing based on random forest classification," *IEEE*, vol. 26, no. 6, pp. 2944–2955, 2021.
- [15] K. Liu, X. Hu, J. Meng, J. M. Guerrero, and R. Teodorescu, "RUBOOST-based ensemble machine learning for electrode quality classification in Li-ion battery manufacturing," *IEEE*, vol. 110 pages, 2021.
- [16] K. Wang, W. Wang, L. Wang, and L. Li, "An improved SOC control strategy for electric vehicle hybrid energy storage systems," *Energies*, vol. 13, no. 20, Article ID 5297, 2020.
- [17] M. K. Azeem, H. Armghan, Z. e. Huma, I. Ahmad, and M. Hassan, "Multistage adaptive nonlinear control of battery-ultracapacitor based plugin hybrid electric vehicles," *Journal of Energy Storage*, vol. 32, Article ID 101813, 2020.
- [18] M. S. Nazir, I. Ahmad, M. J. Khan, Y. Ayaz, and H. Armghan, "Adaptive control of fuel cell and supercapacitor based hybrid electric vehicles," *Energies*, vol. 13, no. 21, Article ID 5587, 2020.
- [19] M. M. Islam, S. A. Siffat, I. Ahmad, M. Liaquat, and S. A. Khan, "Adaptive nonlinear control of unified model of fuel cell, battery, ultracapacitor and induction motor based hybrid electric vehicles," *IEEE Access*, vol. 9, pp. 57486–57509, 2021.
- [20] F. Eroğlu, M. Kurtoğlu, and A. M. Vural, "Bidirectional DC-DC converter based multilevel battery storage systems for electric vehicle and large-scale grid applications a critical review considering different topologies, state-of-charge balancing and future trends," *IET Renewable Power Generation*, vol. 15, no. 5, pp. 915–938, 2021.
- [21] M. Bortoluzzi, C. Correia de Souza, and M. Furlan, "Bibliometric analysis of renewable energy types using key performance indicators and multicriteria decision models," *Renewable and Sustainable Energy Reviews*, vol. 143, Article ID 110958, 2021.
- [22] M. S. Miah, M. S. Hossain Lipu, S. T. Meraj et al., "Optimized energy management schemes for electric vehicle applications a bibliometric analysis towards future trends," *Sustainability*, vol. 13, no. 22, Article ID 12800, 2021.
- [23] A. Katnapally, U. B. Manthathi, A. Chirayarukil Raveendran, and S. Punna, "A predictive power management scheme for hybrid energy storage system in electric vehicle," *International Journal of Circuit Theory and Applications*, vol. 49, no. 11, pp. 3864–3878, 2021.

- [24] J. Fang, H. Deng, N. Tashakor, F. Blaabjerg, and S. M. Goetz, "State-space modeling and control of grid-tied power converters with capacitive/battery energy storage and grid-supportive services," *IEEE Journal of Emerging and Selected Topics in Power Electronics*, vol. 19, pp. 1–17, 2021.
- [25] I. S. Sorlei, N. Bizon, P. Thounthong et al., "Fuel cell electric vehicles—a brief review of current topologies and energy management strategies," *Energies*, vol. 14, no. 1, pp. 252–262, 2021.
- [26] H. Moradisizkoochi, N. Elsayad, and O. A. Mohammed, "A voltage-quadrupler interleaved bidirectional DC-DC converter with intrinsic equal current sharing characteristic for electric vehicles," *IEEE Transactions on Industrial Electronics*, vol. 68, no. 2, pp. 1803–1813, 2021.